

## RESEARCH ARTICLE

View Article Online  
View Journal | View IssueCite this: *Mater. Chem. Front.*, 2021,  
5, 1971

## Understanding the self-ordering of amino acids into supramolecular architectures: co-assembly-based modulation of phenylalanine nanofibrils†

Prabhjot Singh,<sup>a</sup> Satish K. Pandey,<sup>b</sup> Aarzoo Grover,<sup>‡</sup> Rohit K. Sharma<sup>Ⓜ</sup> and Nishima Wangoo<sup>Ⓜ</sup>\*<sup>d</sup>

Amino acids have emerged as promising molecular frameworks for the generation of functional materials owing to the bio-compatibility and thermodynamic stability of their self-assembled architectures. The homogeneous and heterogeneous self-assembly of all naturally occurring amino acids may demonstrate vast functional diversity owing to their common zwitterionic motif, which can serve as a library for the generation of nano/microscale supramolecular biomaterials. Furthermore, amino acids-based self-assembled amyloid structures exhibit pathological relevance, which shifts the paradigm from the self-assembly of polymeric entities to the self-assembly of simple organic molecules or metabolites. Thus, in order to understand the in-built self-ordering behaviour of amino acids, we investigated all naturally occurring amino acids (except aromatic amino acids) for their well-defined morphology and solution-phase  $\beta$ -sheet-like amyloid characteristics. Furthermore, this comprehensive analysis of self-assembly data led to the discovery of aliphatic chain amino acids (ACAAs; Ala, Leu, Ile and Val) as potential candidates for the modulation of phenylalanine fibril toxicity. Thus, this inclusive amino acid self-assembly analysis may pave the way for the design and development of simple organic molecules with inherited self-assembling properties for the generation of functional nanomaterials.

Received 6th October 2020,  
Accepted 21st December 2020

DOI: 10.1039/d0qm00784f

rsc.li/frontiers-materials

## Introduction

The self-assembled architecture made up of small molecular motifs are recognized as the functional force of living systems.<sup>1,2</sup> The optimum balance between intermolecular non-covalent forces to acquire structural diversity and functionality may be identified as the first step towards cellular life.<sup>3</sup> Inspired by this, the molecular self-assembly of supramolecular entities, such as proteins, peptides, DNA and lipids, has been investigated in much detail to understand the mechanism that regulates and controls the matter flux responsible for the functional aspects of living systems.<sup>4</sup> Specifically, self-assembled supramolecular

structures of peptides and proteins have been studied in much detail due to their propensity to form amyloid aggregates.<sup>5–7</sup>

Despite this, limited efforts have been made to understand the well-ordered secondary structures formed by small molecules through the available set of non-covalent forces.<sup>8,9</sup> However, recent reports have suggested a probable link between the self-assembly of metabolites (such as amino acids and nucleotides) and amyloid-based pathological disorders.<sup>10–15</sup> In particular, phenylalanine, tyrosine and adenine structures exhibit amyloid-like toxicity and have been further analyzed for the antibody generation. The mechanism behind many unexplained pathological disorders have been linked to generic  $\beta$ -sheet-type amyloid formation regardless of their molecular origin.<sup>16</sup> In addition, proteins with  $\alpha$ -helix structures have been reported to display amyloid formation, which extends the complexity of these pathogenic structures.<sup>17,18</sup> The occurrence of these pathogenic structures has been linked to serious health problems, such as Alzheimer's, Parkinson's, Chronic Traumatic Encephalopathy (CTE) and phenylketonuria (PKU).<sup>19,20</sup> The occurrence of a high phenylalanine concentration in the blood and observation of phenylalanine self-assembled fibrils in the parietal cortex brain tissue have been recognized as diagnostic tools for PKU.<sup>12,21</sup> To date, tetrahydrobiopterin with a restricted phenylalanine diet has been used as a treatment for patients suffering

<sup>a</sup> Centre for Nanoscience and Nanotechnology, Panjab University, Sector 25, Chandigarh, 160014, India<sup>b</sup> Central Scientific Instruments Organization, Sector-30C, Chandigarh-160030, India<sup>c</sup> Department of Chemistry & Centre for Advanced Studies in Chemistry, Panjab University, Sector 14, Chandigarh-160014, India<sup>d</sup> Department of Applied Sciences, University Institute of Engineering and Technology (U.I.E.T.), Panjab University, Chandigarh-160014, India.

E-mail: nishima@pu.ac.in

† Electronic supplementary information (ESI) available. See DOI: 10.1039/d0qm00784f

‡ Department of Chemistry, University of Vermont, Burlington, Vermont-05405, USA.

from PKU.<sup>22</sup> Further, branched chain amino acids have been clinically adopted as a dietary therapy approach, which is believed to inhibit phenylalanine transport across the blood–brain barrier.<sup>23</sup> However, the mechanistic of branched chain amino acids to lower the adverse health effects in PKU is still unclear.<sup>24</sup>

In this regard, various attempts have been made to understand the self-assembly mechanism of phenylalanine so that it can be used to devise an effective strategy to inhibit its amyloid formation for different motifs, mainly by inhibiting the  $\pi$ – $\pi$  stacking interaction, which is generic in amyloids containing an aromatic residue.<sup>25–31</sup> In our earlier report, we investigated the role of the zwitterionic part in the self-assembly of aromatic amino acids using dielectric modulation of the solvent system.<sup>32</sup> Observed shifts in morphological patterns were suggested to be correlated with the electrostatic interactions between zwitterionic ends in varying dielectric solvents. Further, aromatic and non-aromatic moieties immobilized over gold nanoparticles were demonstrated to have a modulating effect on the self-assembly of aromatic amino acids.<sup>33</sup> Successively, we reported the formation of a phenylalanine dimer assembly nanostructure as the basic building block of amyloids forming nanofibrils, which have been suggested to be responsible for the nerve cell damage in patients suffering from PKU.<sup>34</sup> Therefore, looking at the role of self-assembled amino acids in various pathological disorders and understanding the molecular level self-assembly mechanism of amino acid motifs, herein, we report the self-assembly of all naturally occurring amino acids (except for aromatic amino acids, which was reported in a previous report) in a variety of nano to microscale organizational habits.<sup>32</sup> It is pertinent to note that we report novel self-assembled structures for all the amino acids (except aromatic, cysteine and methionine) for the first time in this paper. This investigation of the self-assembled pattern generation for all amino acids was divided into five categories based on their hydration potential as well as hydrophobicity index. Specifically, the self-assembled architectures for glycine (Gly), alanine (Ala), leucine (Leu), isoleucine (Ile), methionine (Met), valine (Val) (fern-like crystallite), proline (Pro) (rod crystallite) and cysteine (Cys) (globular floral) were reported in category I; threonine (Thr) (spear-like crystallite) and serine (Ser) (capsule structure) in category II; asparagine (Asn) and glutamine (Gln) (dendritic floral) in category III; aspartic acid (Asp) and glutamic acid (Glu) (membrane-like structure) in category IV; lysine (Lys) (microrod crystallite), and arginine (Arg) (nanorod crystallite) and histidine (His) (fibril) in category V were investigated under an optimum set of conditions using optical and field emission scanning electron microscopy (FE-SEM). The observed self-assembled architectures in these categories indicated the occurrence of an inherited structure–morphology relationship for amino acids that may pave the way for the development of the first of its kind of systematic nanofabrication tool using simple organic molecules. Furthermore, all amino acids were investigated for the amyloid characteristics using an optimized aqueous medium thioflavin T (ThT) assay.

The morphological assessment of all the self-assembled amino acids and the presence of a common zwitterionic motif

in monomers inspired us to investigate the role of the co-assembly (in binary mixture) of various amino acids to inhibit phenylalanine fibril formation. Remarkably, aliphatic chain amino acids (ACAAs; Ala, Leu, Ileu and Val) demonstrated a peculiar hindrance to the phenylalanine fibril formation. Furthermore, solution-phase ThT assay for the co-assembled system indicated there was an inhibition of the  $\beta$ -sheet-like structure formation as displayed by phenylalanine. Further, validation of the inhibitory effect exhibited by the co-assembly of ACAAs to reduce phenylalanine cytotoxicity was carried out by using the MTT assay. These intriguing results clearly confirmed the inhibitory role played by ACAAs in regulating the amyloid formation of phenylalanine. Thus, understanding amino acid self-assembly based on microscopic analysis led to the first-of-its-kind molecular structure–morphology pattern relationship. Furthermore, comprehensive analysis of amino acid self-assembly depicted the role of ACAAs in the disruption of phenylalanine fibril formation, which is notable evidence supporting the potential of dietary therapy to work against phenylketonuria.<sup>35</sup>

## Materials and methods

### Materials

All the  $\alpha$ -amino acids were purchased from Sigma-Aldrich and used as such. Milli-Q water (resistivity  $\sim 18.2$  M $\Omega$ ) used for all the self-assembly experiments. The methanol used for the self-assembly experiments was of analytical grade with  $>99\%$  purity.

### Optical microscopy

Optical images of the amino acid self-assembled structures were captured using a light microscope with an in-built camera attachment by depositing 10  $\mu$ L of the sample solution on a microscopic glass slide.

### FE-SEM analysis

FE-SEM was used to investigate the morphology of the self-assembled structures. In general, a 10  $\mu$ L solution of amino acid solution at 1 mg mL<sup>−1</sup> concentration was evaporated slowly on the smooth surface of a Ag film pasted on the FE-SEM step. Pt coating was applied on the samples to make them conductive, followed by FE-SEM analysis on a Hitachi, SU8010 electron microscope, operating at 10–15 kV.

### Confocal laser scanning microscopy

The fluorescence emission signal in the ThT binding assay as well as the intrinsic emission of the self-assembled structures were captured using the Zeiss LSM 510 confocal laser scanning microscope. In general, the samples were prepared by air drying 10  $\mu$ L of each sample solution on a microscopic glass slide.

### Fluorescence spectroscopy

The fluorescence spectra were recorded on an Agilent Technologies Cary Bundle instrument. For ThT optimization, various concentrations varying from 0.0001 to 1.0000 mg mL<sup>−1</sup> were prepared in an aqueous medium and the fluorescence spectra recorded at an

excitation wavelength of 370 nm. For ThT assay, ageing of the amino acid solutions (concentration 80 mM) were done by placing them in a closed vessel and leaving undisturbed at room temperature for 15 days, followed by the addition of optimized ThT concentration (2.5  $\mu\text{M}$ ) for the binding assay. The solution-phase ThT binding assay for all the amino acids was performed using optimized ThT as the final concentration in the sample solutions.

### Cell viability assay

The cell cytotoxicity of the amino acid samples was assessed against HeLa cells *via* a 3-(4,5)-dimethylthiazol-2-yl)-2,5-diphenyl tetrazolium bromide (MTT) assay. Briefly, HeLa cells were seeded ( $2 \times 10^4$  cells per well) in triplicate in a 96-well culture plate containing RPMI-1640 (supplemented with 5% fetal bovine serum) and incubated for 24 h. Cells were treated with amino acid self-assembled structures at different concentrations for the cytotoxicity assay. After the required duration, the medium was aspirated and 100  $\mu\text{L}$  fresh medium was added to each plate. Thereafter, the cells were treated with 20  $\mu\text{L}$  of MTT solution (2.5  $\text{mg mL}^{-1}$  in PBS) and again left to incubate for 4 h at 37  $^\circ\text{C}$ . The supernatant was separated and the resulting formazan crystals were dissolved in 100  $\mu\text{L}$  DMSO. The samples were measured for their absorbance at 570 nm with a microplate reader. The comparative viability of cells was calculated by the O.D. 570 ratio of the treated and untreated cells.

## Result and discussion

The amyloid-like self-assembled fibril morphology of aromatic amino acids inspired us to perform a comprehensive investigation of the patterned structures for all naturally occurring amino acids. Moreover, the occurrence of a common zwitterionic motif in all the natural amino acids and its indispensable role in determining the self-assembly of amino acids was an added motivation behind this comprehensive investigation.<sup>36,37</sup> In this regard, we analyzed the self-assembly of all naturally occurring amino acids (except aromatic amino acids) by dividing them into

five categories depending on their hydration potential as well as hydrophobicity index.<sup>38–40</sup>

### Category I: self-assembly of glycine and amino acids with a neutral side chain (Gly, Ala, Val, Leu, Ile, Cys, Met)

Considering the properties of amino acids, such as their hydration potential as well as hydrophobicity index, allowed us to devise a strategy to organize all naturally occurring amino acids (except aromatic amino acids) into five categories with a gradual change of properties from a low hydration potential and high hydrophobicity index (category I) to high hydration potential and low hydrophobicity index (category V) [ESI,† Table S1].

Based on this rationale, the self-assembly of glycine (Gly), alanine (Ala), leucine (Leu), isoleucine (Ile), valine (Val), proline (Pro), methionine (Met) and cysteine (Cys) was investigated in category I amino acids [Fig. 1(a–h)]. For this purpose, amino acid solutions were prepared in a water and methanol:water (1 : 1) [MW 1.1] solvent system and their self-assembled patterns were observed using optical microscopy and FE-SEM. Remarkably, glycine, ACAAs (Ala, Leu, Ile, Val) and methionine (Met) displayed the formation of exceptionally similar self-assembled patterns forming micro-crystallite structures arranged in fern-like architectures in both water and [MW 1.1] solvent as evident by the optical microscopy and FE-SEM results [Fig. 1(a–f) and ESI,† Fig. S1–S6].

The formation of a fern-like crystallite for glycine may be solely due to the inter-zwitterionic interactions. In a recent report, the formation of similar needle-like micro crystals for glycine displayed a high piezoelectric coefficient of magnitude equivalent to barium titanate or lead zirconate titanate.<sup>41</sup>

The occurrence of common micro-crystallite structures demonstrated the ability of zwitterionic interactions to play a dominant role in the molecular recognition in the self-assembly of category I amino acids as depicted by the tightly packed inter-zwitterionic interactions in the single-crystal structures of these amino acids.<sup>36</sup> Remarkably, isoleucine, one of the lowest soluble (34  $\text{mg mL}^{-1}$ ) aliphatic amino acid in water, exhibited restricted crystalline growth to form a

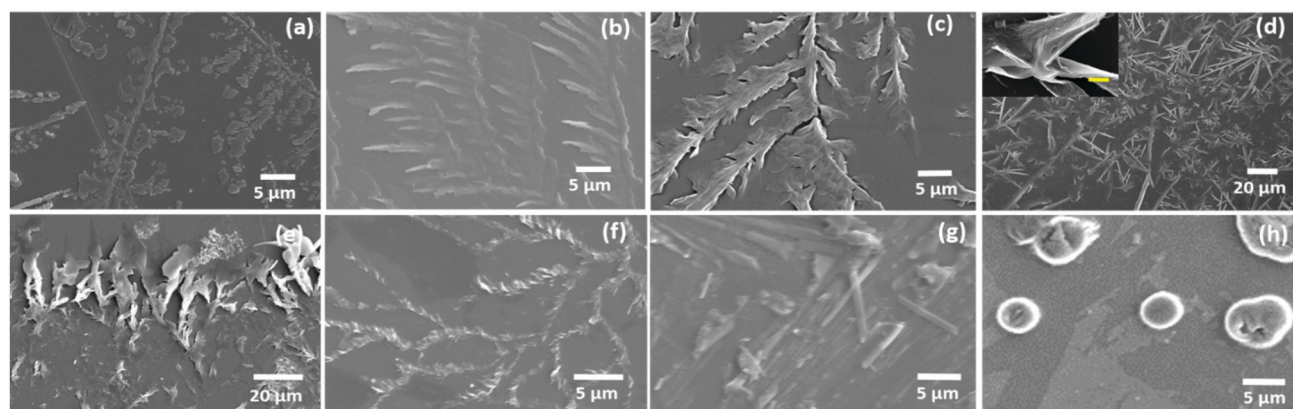


**Fig. 1** FE-SEM images of Gly (a), Ala (b), Leu (c), Ile (d), Val (e), Met (f), Pro (g) displaying the formation of microcrystals arranged in fern-like architectures, and Cys (h) displaying the formation of globular structures [ESI,† Table S2 for specific set of conditions].



nano-sized curved sheet-like morphology approximately 100 nm wide in the MW 1.1 solvent system [Fig. 1d inset, scale bar 400 nm]. The nanodimensional order observed in the case of the isoleucine self-assembled structures suggested that van der Waals interactions between the aliphatic side chain may also play a decisive role in controlling the crystallinity along with the zwitterionic dipolar hydrogen bonds interaction.

The self-assembly of proline did not display any ordered self-assembled architecture at 1 mg mL<sup>-1</sup> concentration, which may be due to its high solubility (1620 mg mL<sup>-1</sup>) in water [ESI,† Fig. S7(a)]. Thus, proline self-assembly was generated using concentration and solvent modulations (5 mg mL<sup>-1</sup> and 80% methanol in water), which led to the formation of micro-rod-type crystallite structures [Fig. 1(g) and ESI,† Fig. S7(b, c)]. Interestingly, the self-assembly of cysteine exhibited globular structures in water and MW 1.1 [Fig. 1(h) and ESI,† Fig. S8]. In addition to globular structures, the optical microscopic images for cysteine also displayed an elongated rod-like morphology, which may be detected as fibril-like structures in recent work exhibiting amyloid-like toxicity.<sup>42</sup> The interesting morphological shift in the case of cysteine from the ACAAs self-assembled structures may be due to weak S–S interactions as depicted by theoretical studies on the intermolecular interactions of chalcogens.<sup>43</sup> Thus, not only the ionic interactions of category I amino acids, but also the van der Waals intermolecular interactions exhibited by the side chain also play a vital role in determining the molecular recognition responsible for the formation of ordered assembly structures.

### Category II: self-assembly of amino acids with an hydroxyl side chain (Thr, Ser)

Threonine and serine have greater hydration potentials (−4.88 and −5.06, respectively) as well as hydrophobicity index values (0.7 and 0.8, respectively) than category I amino acids [ESI,† Table S1]. The self-assemblies of threonine and serine were investigated in category II using a water and MW 1.1 solvent system [ESI,† Fig. S9 and S10]. Interestingly, threonine displayed an aligned spear-like structure of identical sizes, as evident through the FE-SEM micrographs [Fig. 2(a) and ESI,† Fig. S9]. The morphological shift from a fern-like structure (category I) to aligned spear-like structure for threonine could be attributed to the introduction of a hydroxyl group in the amino acid side chain. Furthermore, the hydroxyl group in the Thr side chain greatly enhanced the solubility of amino acids from ~35 mg mL<sup>-1</sup> (Ile) to ~97 mg mL<sup>-1</sup> (Thr), which further depicted the ability of threonine to exhibit polar interactions, which may have provided directionality to the self-assembled micro-crystallite structures as visualized by the FE-SEM images. On the other hand, self-assembly analysis of freshly prepared serine at 1 mg mL<sup>-1</sup> exhibited the layer formation in FE-SEM micrograph [ESI,† Fig. S10(a)]. The observed deposited layer may be due to extensive solute–solvent interactions owing to the high solubility (425 mg mL<sup>-1</sup>) of serine in water. Thus, in order to eliminate the solvent and to visualize the structures, self-assembly was performed at 50 °C with an incubation period of 24 h. Interestingly, serine was observed to form orderly

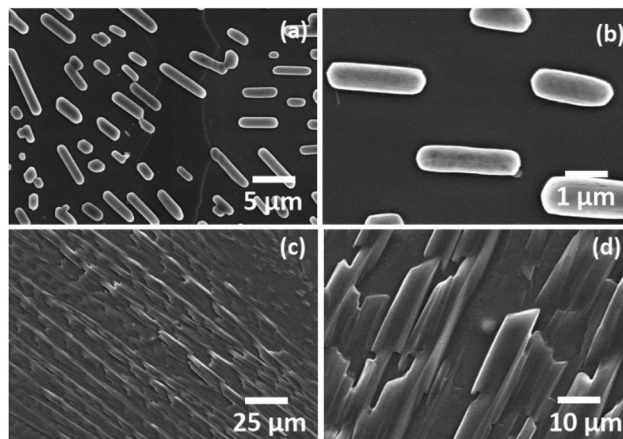


Fig. 2 FESEM images depicting the self-assembled architectures of Ser (a and b) and Thr (c and d) using water as the solvent.

aligned capsule-shaped structures both in water and in the MW 1.1 solvent system [Fig. 2(b) and ESI,† Fig. S10 (b, c)]. The hierarchy of the architectural shift from micro-crystalline (Category I) to orderly spear-like crystals (Thr) (Category II) to formation of a capsule-like morphology (Ser) points towards the inherent structure–morphology relationship for self-assembled amino acids.

### Category III: self-assembly of amino acids with an amide linkage in the side chain (Gln, Asn)

The amide bond is the most abundant chemical linkage in biological systems and provides rigidity and directionality to the protein and peptide secondary structures.

Consequently, the self-assembly analysis of asparagine (hydration potential, −9.68 and hydrophobicity index −3.5) and glutamine (hydration potential, −9.38 and hydrophobicity index, −3.5) were performed in category III using water and MW 1.1 as the solvent system. The self-assembled structures of both glutamine and asparagine displayed the formation of floral dendritic assemblies with a stacked fibrillary network showing a drastic morphological shift from category I and category II amino acids [Fig. 3(a, b) and ESI,† Fig. S11, S12].

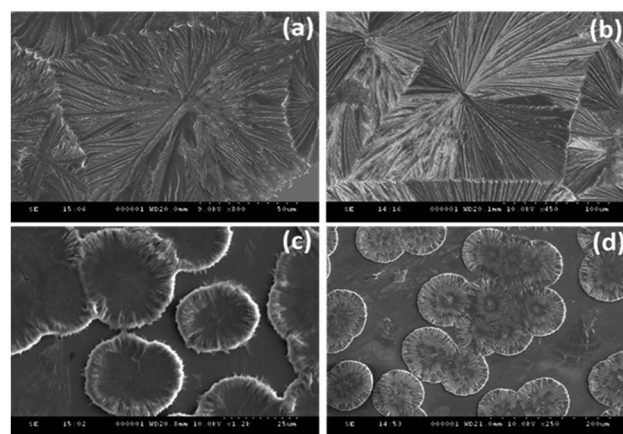


Fig. 3 FE-SEM images depicting the self-assembled architectures of Gln (a), Asn (b), Glu (c) and Asp (d).

This morphological shift may be correlated to the increase in side chain polar interactions as evident from the hydration potential data [ESI,† Table S1].

#### Category IV: self-assembly of amino acids with a carboxylic group in the side chain (Glu, Asp)

The self-assembly analysis was continued for amino acids with carboxylic acid in the side chain using water and MW 1.1 solvent system. The self-assembly analysis of glutamic acid and aspartic acid was performed in various solvent systems [ESI,† Fig. S13(a–c)] and S14(a–c)]. The observed micrographs revealed the formation of membrane-like structures for glutamic acid in water and 0.1 M HCl whereas aspartic acid displayed similar membrane-like architectures in 0.1 M aqueous ammonia solution. The outer layer of membrane-like morphology for glutamic acid and aspartic acid structures displayed inter-structural diffusion as depicted by FE-SEM images which indicated the soft and permeable nature of these higher order assemblies [Fig. 3(c and d)]. The formation of completely different self-assembled architectures for category IV may be attributed to the higher value of hydration potential (Glu =  $-10.20$ ; Asp =  $-10.95$ ) and hydrophobicity index (Glu =  $-3.5$ ; Asp =  $-3.5$ ) as compared to category I to III amino acids which indicated increase in polarity of side chain. Despite higher hydration potential, category IV amino acids exhibited low solubility in water (Asp  $\sim 5$  mg mL $^{-1}$  and Glu  $\sim 8$  mg mL $^{-1}$ ) that may be due to decreased solute–solvent interactions. Therefore, the formation of such well-ordered membrane-like architectures may be due to optimum balance between inter-side-chain interactions depicted by higher value of hydration potential and low water solubility in water.

At this stage, a conceptual hypothesis can be introduced based on the intriguing results, which may give a primitive and first-of-its-kind description of the structural–morphological relationship for amino acid self-assembly. The gradual shift in the self-assembled morphology from category I (crystallite) to

category IV (soft membrane) amino acids with the increase in hydration potential value strengthens the possibility of performing an impeccable molecular design linked to the fabrication of nano/microscale architectures [Fig. 4].

The self-assembly analysis of amino acids in aqueous media with varying degrees of dielectric constant indicated that zwitterionic dipolar interactions play a dominating role in imparting ionic crystallinity to supramolecular structures. The high order morphology generated by these ionic interactions may be termed as hard crystallinity, which seldom is affected by slight changes in the side chain van der Waals interactions as displayed by category I amino acids. On the other hand, an increase in the contribution of inter-side-chain polar interactions between amino acid monomers may shift the morphology from hard crystallinity to soft crystallinity as depicted by the morphological trends from category II to category IV amino acids.

#### Category V: self-assembly of amino acids with a cationic moiety in the side chain (Lys, His and Arg)

The amino acids with a cationic side chain (hydration potential for Lys, His and Arg are  $-9.52$ ,  $-10.27$  and  $-19.92$ , respectively) exhibited very high solubility in water. This behaviour may be responsible for the suppression of the intermolecular recognition and thereby may impose a restriction on the formation of ordered assembly structures [ESI,† Fig. S15].

Therefore, pH modulation was done for self-assembly generation of the cationic amino acids. The self-assembly of lysine was done using 0.1 M NaOH, and it displayed elongated assemblies, which were also visualized as exhibiting an aligned perpendicular growth over the surface [Fig. 5(a and b)].

Further, arginine displayed nanoscale rod-like crystallinity, which grew to form snowy flake-type structures in 0.1 M aqueous NaOH solution [Fig. 5(c and d)]. The solubility of histidine is higher than the other aromatic amino acids, which may be one of the reasons behind the inability of histidine to show

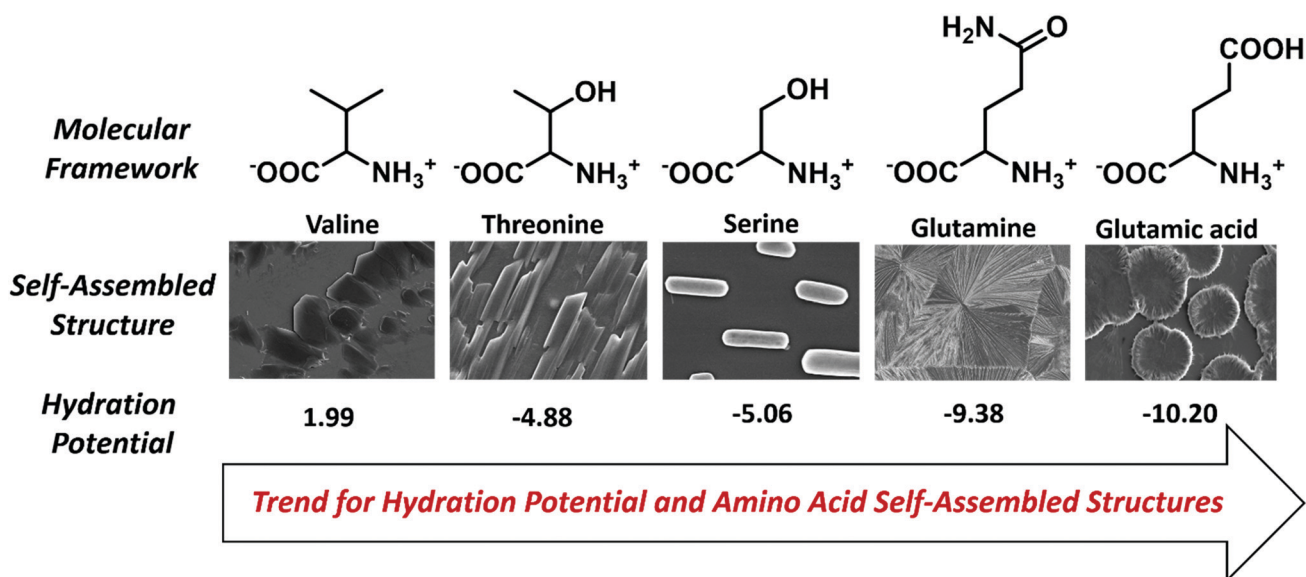


Fig. 4 Pictorial description of the hydration potential trend and structural–morphological shift for amino acid self-assembled architectures.

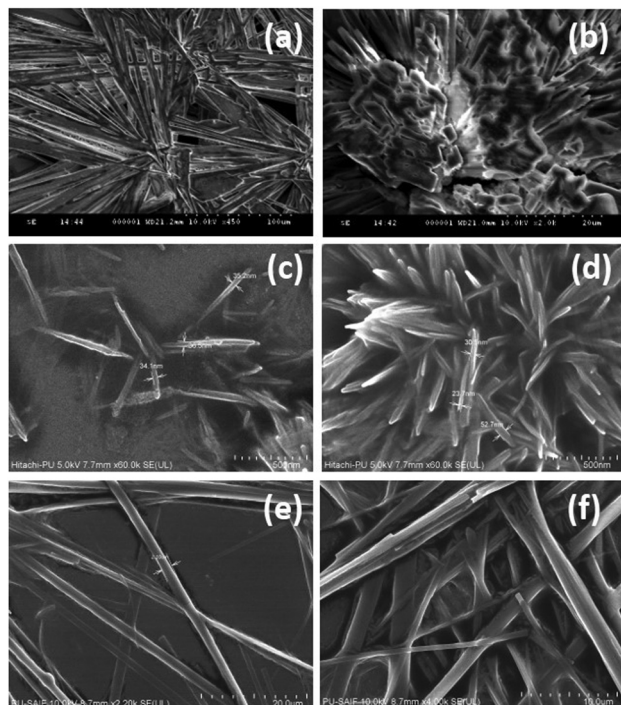


Fig. 5 FE-SEM images depicting the self-assembled architectures of Lys (a and b), Arg (c and d) and His (e and f).

$\pi$ -stacking-based fibril formation. In this regard, the self-assembly of histidine was performed in basic medium (pH 8 using NaOH) using a water and methanol:water (1 : 1) solvent system [Fig. 5(e and f)]. Remarkably, histidine demonstrated the formation of a long-range fibril morphology in the basic medium. Thus, in-depth analysis of the structure–morphological relationship under varying conditions led us to modulate the histidine self-assembled architectures from dendritic rod structures to fibrils.<sup>32</sup>

Thus, all the naturally occurring amino acids displayed the formation of highly ordered self-assembled architectures under optimum conditions, which represents the uniqueness of their molecular framework. The structure–morphology relationship of amino acids can be explored to fabricate controlled but diverse nano or microscale materials using synthetic organic chemistry.

### Investigation into the amyloid characteristics exhibited by all naturally occurring amino acids

**Optimization of ThT concentration for achieving the maximum emission intensity in water.** The formation of amyloid aggregates acts as a strong trigger for the occurrence of many neurodegenerative disorders.<sup>6</sup> Thus, it is highly crucial to investigate the amino acid-based self-assembled structures for amyloid formation, which may be useful to understand their formation mechanism, diagnosis and treatment. The detection of amyloid structures is mainly done by ThT fluorescence assay. ThT is a small molecular dye, which displays an enhancement in its fluorescence signal upon binding to amyloid aggregates.<sup>44</sup> The enhancement in fluorescence intensity has been attributed to the immobilization

of the central C–C bond between benzothiazole and aniline rings.<sup>45</sup> Furthermore, it has been reported that at least four  $\beta$ -strands have to be present for the binding of ThT to the channels along the long axis of amyloid fibrils. As organic dyes are susceptible to exhibiting excimer-based fluorescence quenching in polar solvents, thus the ThT concentration was optimized prior to the amino acid amyloid characterization in aqueous medium.<sup>46</sup> For this purpose, the fluorescence spectrum of ThT was examined at different aqueous concentrations varying from 0.1 to 1.0 mg mL<sup>-1</sup> at an excitation wavelength of 370 nm [ESI,† Fig. S16]. ThT solution with 0.5  $\mu$ g mL<sup>-1</sup> concentration displayed the maximum fluorescence intensity, suggesting it would be suitable for the characterization of single amino acid-based amyloid structures in aqueous media.

**Optimization of the phenylalanine concentration and investigating solution-phase amyloid formation for all naturally occurring amino acids.** The amyloid formation of biological agents depends strongly on the molecular motif as well as on the set of solvothermal conditions, such as pH, concentration, temperature and solvent system.<sup>47</sup> These varying conditions make it quite challenging to perform a comprehensive analysis of amyloid formation by all naturally occurring amino acids. Thus, in order to minimize the state factors, various factors, such as neutral pH, water as a solvent and room temperature, were kept constant for all the measurements. Furthermore, phenylalanine was selected as a model amyloid forming amino acid in aqueous medium with respect to the considerable literature on the same.<sup>48</sup> Initially, the phenylalanine concentration was optimized for obtaining the required ThT response. For this purpose, phenylalanine at varying concentrations ranging from 0.20 mg mL<sup>-1</sup> (1.2 mM) to 15 mg mL<sup>-1</sup> (90 mM) was analyzed using ThT assay, which showed a gradual increase in the fluorescence intensity, indicating the formation of  $\beta$ -sheet structures [ESI,† Fig. S17]. However, keeping in mind the aqueous solubility, 80 mM concentration was selected for the detection of amyloid formation for all naturally occurring amino acids. Thus, the amyloid-like structural formation for amino acids in water was performed at optimized parameters of 0.8  $\mu$ g mL<sup>-1</sup> (2.5  $\mu$ M) final ThT concentration and 80 mM final amino acid concentration in aqueous medium with a neutral pH at room temperature. Initially, the prepared aqueous solutions were heated at 90 °C for 5 min to completely solubilize the amino acids monomers, which were then incubated for 15 days (ageing) for the generation of the amino acid self-assembled structures. The optimized ThT solution was then added to the matured self-assembled architectures and a 48 h agitation was introduced prior to obtaining the fluorescence spectra at 370 nm excitation wavelength. The results depicted a considerable rise in the ThT fluorescence intensity for phenylalanine, tryptophan, tyrosine, asparagine and cysteine [Fig. 6]. The validation of this method can be found in the fact that all the previously reported amyloid forming amino acids, such as phenylalanine, tryptophan, tyrosine and cysteine displayed, the same specific  $\beta$ -sheet signature obtained in the present optimization. In addition to this, asparagine and histidine also demonstrated the formation of  $\beta$ -sheet amyloid structures. Thus, not



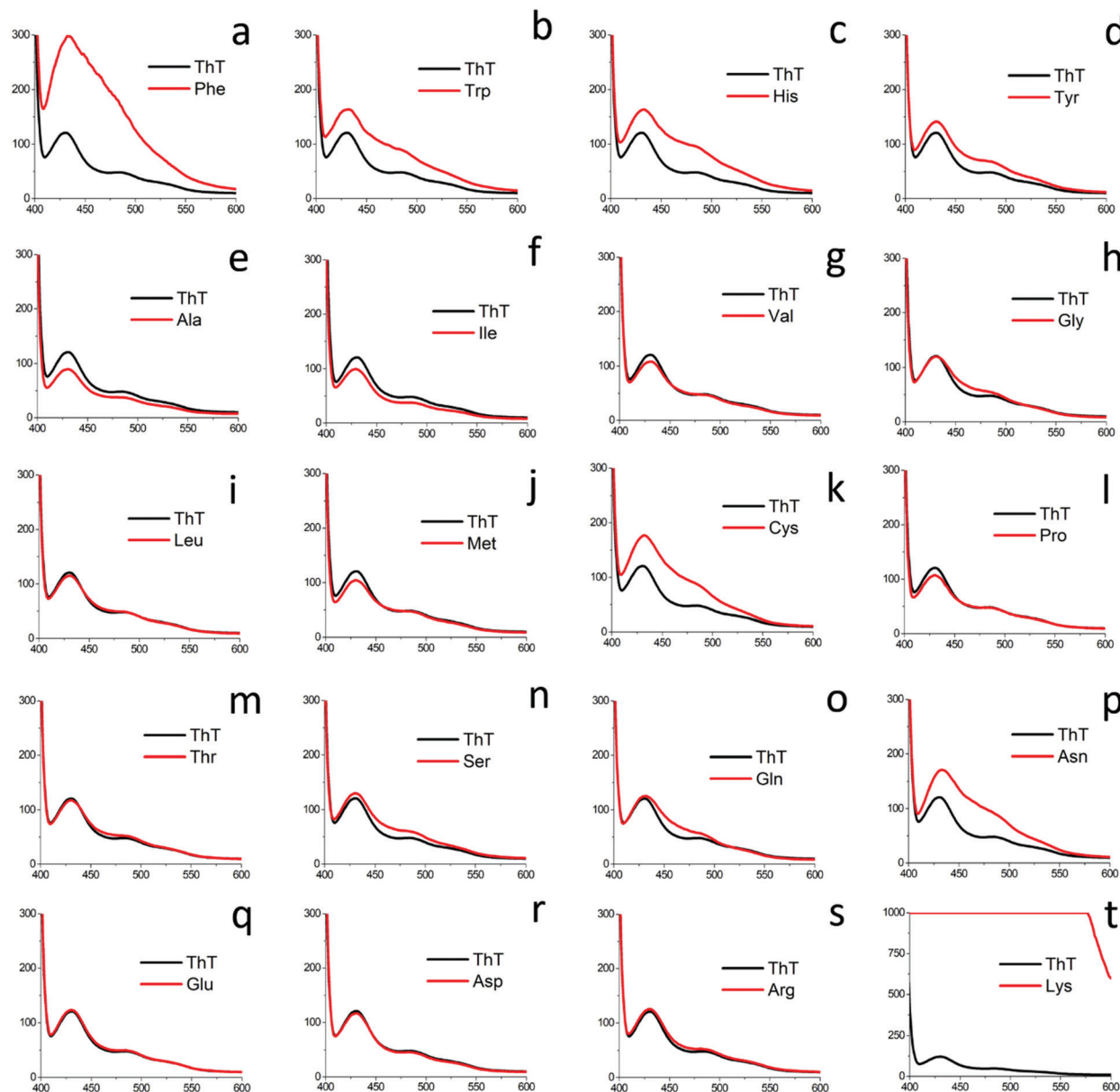


Fig. 6 ThT fluorescence assay for all naturally occurring amino acids at 80 mM concentration using optimized ThT concentration.

only phenylalanine, but other metabolites such as amino acids may also accumulate under specific conditions to form amyloid-like aggregates.

**Investigation of asparagine amyloid characteristics.** Investigation of the solution-phase amyloid formation for all amino acids using ThT assay displayed the propensity of asparagine to form  $\beta$ -sheet-like architectures. So far, asparagine-rich regions have been demonstrated to enhance the formation of pathogenic protein aggregates.<sup>49</sup> However, to the best of our knowledge, no report has yet mentioned the accumulation of single asparagine to form amyloid-like characteristics. Thus, morphological analysis of asparagine was investigated in detail using optical microscopy, FE-SEM and CLSM [Fig. 7(a-c)]. In all the micrographs, asparagine displayed the formation of a fibrillary architecture arranged in a floral dendritic fashion, which

confirmed its ability to form well-ordered supramolecular structures.

Further, asparagine exhibited a concentration-dependent enhancement in  $\beta$ -sheet formation in aqueous medium as depicted by the ThT assay [Fig. 7(d)]. The specific binding of ThT with asparagine self-assembled patterns was further confirmed by CLSM analysis [Fig. 7(e)]. Finally, the cytotoxicity analysis of the asparagine self-assembled structures was validated by MTT assay, which showed up to 50% cell death at a saturated concentration ( $30 \text{ mg mL}^{-1}$ ) of asparagine in water [Fig. 7(f)]. Thus, the comprehensive self-assembly analysis of all naturally occurring amino acids provided valuable information regarding the asparagine amyloid-like behaviour that may be one of the missing links in understanding prion-based pathological disorders.

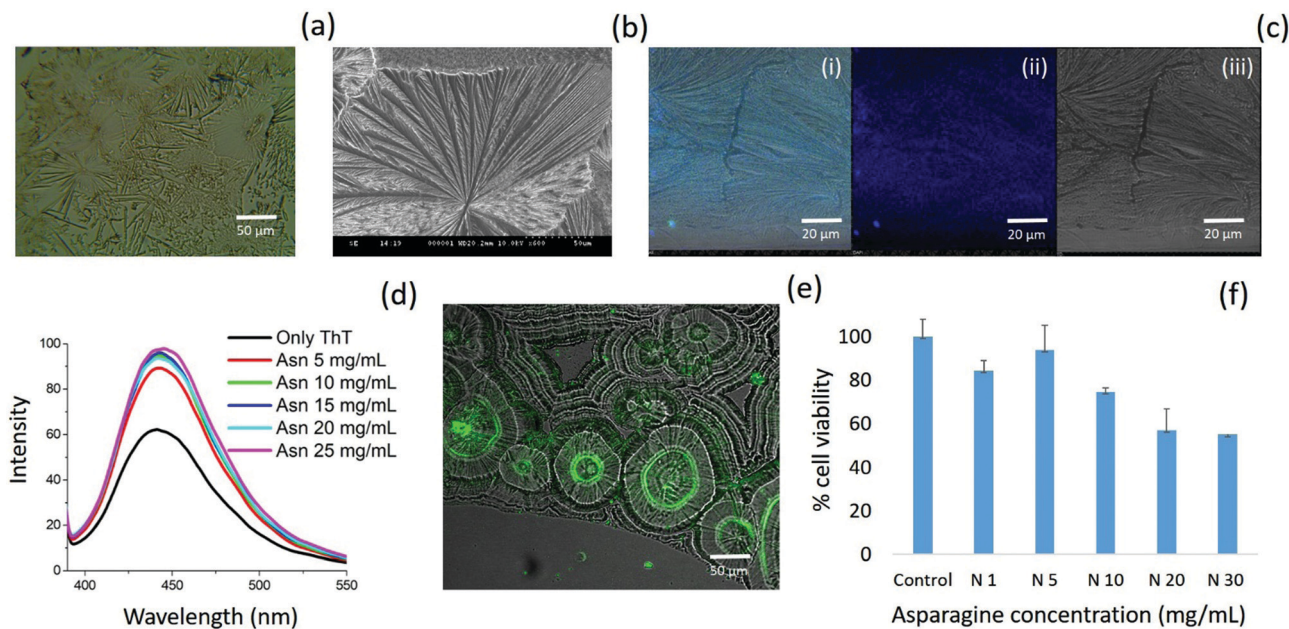


Fig. 7 Asparagine self-assembled structures using optical microscopy (a); FE-SEM (b); CLSM (c); ThT fluorescence for asparagine self-assembled structures in aqueous medium (d); deposited phase ThT binding assay for asparagine (e); cytotoxicity assay for asparagine self-assembled structures using MTT assay (f).

### Application towards the anti-amyloid approach against phenylketonuria

Our inclusive analysis of amino acid self-assembled structures in water and MW solvent system provided valuable insights into the role of zwitterionic and side chain intermolecular interactions in determining the structural-morphological relationship. This understanding may have wide implications in various fields, such as for the development of therapeutics for metabolite amyloids, bioinspired materials design and the generation of multi-component ordered assemblies. The *category I* amino acids displayed the formation of a fern-like crystallite structure, which may have been driven mainly *via* electrostatic inter-zwitterionic interactions. Recently, efforts have been made to explore co-crystallization to synergistically expand the structural complexity of amino acid-based supramolecular structures.<sup>8</sup> Thus, an amino acid co-assembly approach based on the new understanding of amino acid interactions *via* a common zwitterionic motif can be utilized to alter the toxicity profile of phenylalanine fibrils. To test this hypothesis, first, the deposited phase co-assembly of phenylalanine with all the amino acids was investigated by optical microscopy [ESI,† Fig. S18–S36]. The phenylalanine fibril pattern was observed to undergo a modification upon co-assembly with ACAAs (Ala, Leu, Ile and Val). Furthermore, this morphological modulation of phenylalanine fibrils was confirmed by electron microscopy [Fig. 8(I)]. Remarkably, the FE-SEM images displayed a transverse growth of microstructures on the longitudinal fibril axis. This peculiar modification of phenylalanine fibrils by the co-assembly of aliphatic amino acid may be due to intermolecular heterogeneous interactions between phenylalanine and ACAAs through the zwitterionic ends.

Furthermore, the modification of phenylalanine fibrils by ACAAs led us to investigate their anti-amyloid action as a modal treatment for PKU. For this purpose, the ThT assay was performed for phenylalanine co-assembled structures with ACAAs at an 80 mM concentration using only phenylalanine as a control [Fig. 8(II)]. The results showed that ThT had a suppressed intensity in the case of the co-assembled states compared to the controlled phenylalanine solution, demonstrating the ability of ACAAs to inhibit the phenylalanine  $\beta$ -sheet-type fibril formation in aqueous media. Furthermore, the deposited phase ThT assay of phenylalanine and valine demonstrated a complete morphological shift from fibril to disc-like aggregates [Fig. 8(III)]. The deposited phase ThT binding assay for the leucine and phenylalanine co-assembled state also demonstrated a decrease in fluorescence intensity, suggesting lower  $\beta$ -sheet characteristics in the co-assembled state [ESI,† Fig. S37]. The modulatory effect the ACAAs displayed on phenylalanine fibrils was correlated with the decrease in cytotoxicity in the co-assembled state when performing *in vitro* cytotoxicity analysis. The results of the MTT assay displayed a considerable decrease in cell toxicity for the phenylalanine:ACAAs co-assembled systems as compared to the phenylalanine-only self-assembled structures [Fig. 8(IV)]. Recently, single amino acid-based ordered assemblies have displayed unique photoluminescent characteristics, which have suggested to be due to a quantum level clustering of hydrogen bond interactions.<sup>34,50–52</sup> In this context, phenylalanine:leucine (1:1) co-assembly revealed a complete morphology shift for phenylalanine fibrils to form spherical structures with unique intrinsic fluorescence emission as visualized by CLSM [Fig. 8(V)]. Thus, morphological analysis, ThT assay and cytotoxicity



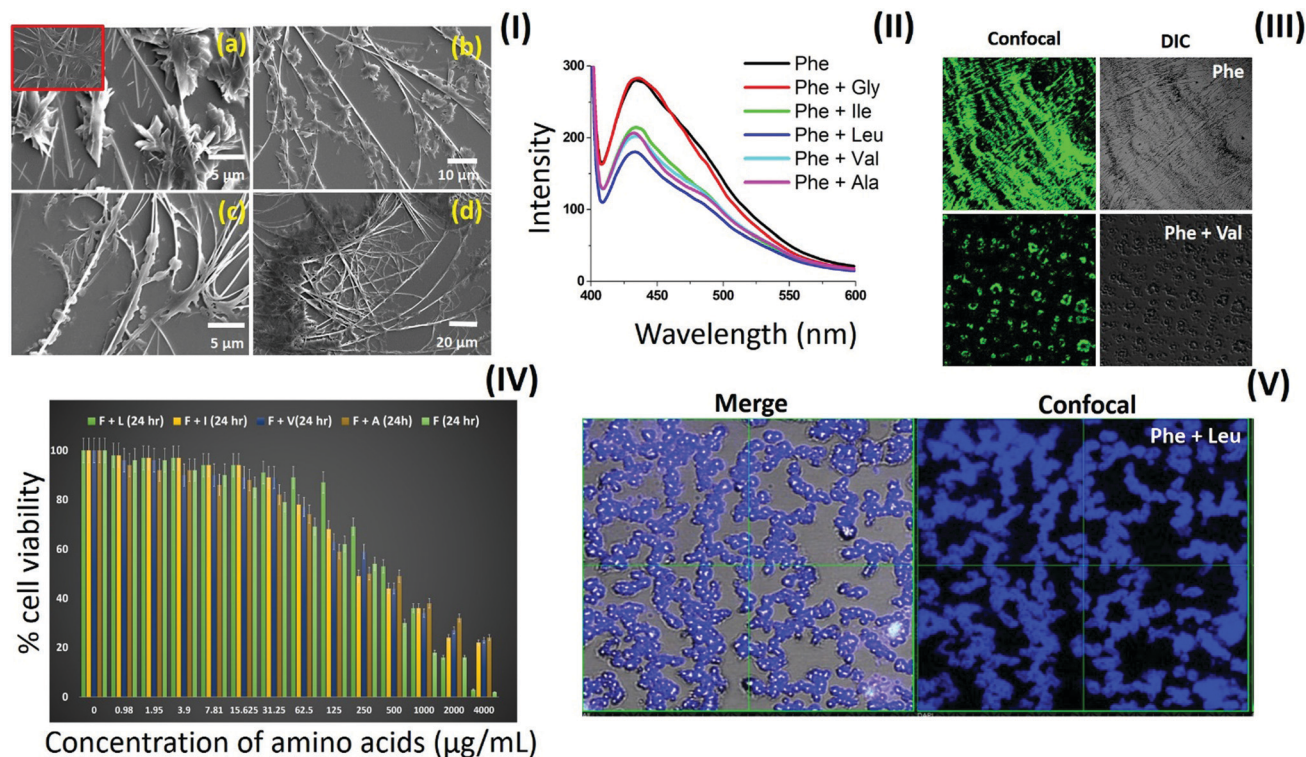


**Fig. 8** FE-SEM images displaying phenylalanine co-assembly with alanine (Ia), isoleucine (Ib), leucine (Ic), valine (Id); ThT assay of the solution-phase co-assembly of phenylalanine with ACAAs (II); Deposited phase ThT binding assay displaying phenylalanine fibril disruption upon co-assembly with valine (III); MTT cytotoxicity assay of co-assembled amino acids using phenylalanine as the control (IV); CLSM image depicting intrinsically fluorescent spherical structures formed by phenylalanine : leucine (1 : 1) co-assembly (V).

analysis confirmed the ability of the ACAAs to modify the phenylalanine fibril assembly in such a way that may be utilized for the treatment of PKU. Furthermore, the peculiar modification of the amyloid characteristics of co-assembled architectures comprising unique intrinsic emission may have potential biotechnological applications. These intriguing results may have wide implications in the design of a preventive strategy against phenylalanine fibril toxicity assembly as well as for the development of multi-component supramolecular structures with improved physical properties.

## Conclusions

The self-assembling analysis for all naturally occurring amino acids in comparable physical conditions have provided much needed understanding about the mode of amino acid molecular recognition that may lead to tailor made design for the nano/microscale self-assembled architectures using synthetic molecules. In particular, Category I amino acids including Ala, Leu, Ileu, Val, and Met demonstrated fern-like crystallite assembly structure which may be owing to the dominating zwitterionic bridging interactions. The self-assembly of serine and threonine (with hydroxyl group in side chain) in Category II displayed the formation of aligned capsule and spear-like structures. Further, the amino acids with amide (Category III; Gln, Asn) and acidic side

chain (Category IV; Glu, Asp) demonstrated the formation of well-ordered floral dendritic and membrane-like structures, respectively. Interestingly, pH modification of amino acid with cationic side chain (Category V; Histidine, Lysine and Arginine) demonstrated the formation of well-defined fibrils for histidine and high aspect ratio structures for lysine and arginine. The investigation of solution-phase  $\beta$ -sheet-like structures using optimized ThT assay demonstrated the amyloid-like etiology for phenylalanine, tyrosine, tryptophan, histidine and cysteine which correlates to the earlier reports. Further, asparagine displayed the formation of  $\beta$ -sheet-like structure for the first time. The asparagine amyloid characteristics was validated using histological, morphological and cytotoxicity assay which further extended the generic amyloid paradigm to the amino acid metabolites. Finally, the understanding of the role of the zwitterionic motif to form bridging interactions and their direct effect on the supramolecular morphology stimulated the heterogeneous co-assembly approach that led to the discovery of ACAAs (Ala, Leu, Ileu, and Val) as anti-amyloid agents for phenylalanine toxic fibrils. The formation of well-defined co-assembled structures also delineated the role of bridging zwitterionic interactions in stabilizing the amino acid supramolecular architectures.

Amino acids as natural building blocks have emerged as a unique molecular library with inherited functional diversity that may be used for the generation of self-assembled functional materials capable of transforming healthcare and energy systems. The ability of heterogeneous molecular recognition displayed by

amino acids may be utilized to tackle the metabolic amyloid aggregation using controlled co-assembly techniques. Furthermore, the in-depth understanding of well-ordered fabrication displayed by amino acids may be vital for the generation of non-amyloidic nanomaterials for biomedical applications. The amino acid self-assembly data may also serve as a guiding tool for the design and synthesis of organic molecules with inherited self-assembling properties. Thus, the present study may pave the way for the controlled fabrication of a new class of nano/microscale biomaterials for diverse biomedical applications.

## CRedit authorship contribution statement

Prabhjot Singh: Writing – original draft, Investigation, Methodology, Conceptualization and Experimentation. Satish K. Pandey: Biological experimentation, Investigation. Aarzo Grover: Experimentation. Rohit K. Sharma: Manuscript editing and Methodology. Nishima Wangoo: Supervision, Conceptualization, Manuscript writing and review, Overall supervision, Research support.

## Data availability

The data required to reproduce these findings can be made available on request.

## Conflicts of interest

There are no conflicts to declare.

## Acknowledgements

This work was supported by Science Engineering and Research Board (SERB) of India grant no. ECR/2017/000874 and DST-PURSE grant awarded to NW. PS thanks University Grant Commission (UGC), India, for his senior research fellowship.

## References

- 1 J. W. Szostak, D. P. Bartel and P. L. Luisi, Synthesizing life, *Nature*, 2001, **409**, 387–390.
- 2 G. M. Whitesides and M. Boncheva, Beyond molecules: Self-assembly of mesoscopic and macroscopic components, *Proc. Natl. Acad. Sci. U. S. A.*, 2002, **99**, 4769–4774.
- 3 P.-A. Monnard and D. W. Deamer, Membrane self-assembly processes: Steps toward the first cellular life, *Anat. Rec.*, 2002, **268**, 196–207.
- 4 B. A. Grzybowski and W. T. S. Huck, The nanotechnology of life-inspired systems, *Nat. Nanotechnol.*, 2016, **11**, 585–592.
- 5 F. Chiti and C. M. Dobson, Amyloid formation by globular proteins under native conditions, *Nat. Chem. Biol.*, 2009, **5**, 15–22.
- 6 C. Soto and S. Pritzkow, Protein misfolding, aggregation, and conformational strains in neurodegenerative diseases, *Nat. Neurosci.*, 2018, **21**, 1332–1340.
- 7 E. Gazit, Self Assembly of Short Aromatic Peptides into Amyloid Fibrils and Related Nanostructures, *Prion*, 2007, **1**, 32–35.
- 8 S. Bera, S. Mondal, Y. Tang, G. Jacoby, E. Arad, T. Guterman, R. Jelinek, R. Beck, G. Wei and E. Gazit, Deciphering the Rules for Amino Acid Co-Assembly Based on Interlayer Distances, *ACS Nano*, 2019, **13**, 1703–1712.
- 9 N. Amdursky and M. M. Stevens, Circular Dichroism of Amino Acids: Following the Structural Formation of Phenylalanine, *ChemPhysChem*, 2015, **16**, 2768–2774.
- 10 S. Shaham-Niv, L. Adler-Abramovich, L. Schnaider and E. Gazit, Extension of the generic amyloid hypothesis to nonproteinaceous metabolite assemblies, *Sci. Adv.*, 2015, **1**, e1500137.
- 11 S. Shaham-Niv, P. Rehak, L. Vuković, L. Adler-Abramovich, P. Král and E. Gazit, Formation of Apoptosis-Inducing Amyloid Fibrils by Tryptophan, *Isr. J. Chem.*, 2017, **57**, 729–737.
- 12 L. Adler-Abramovich, L. Vaks, O. Carny, D. Trudler, A. Magno, A. Caflisch, D. Frenkel and E. Gazit, Phenylalanine assembly into toxic fibrils suggests amyloid etiology in phenylketonuria, *Nat. Chem. Biol.*, 2012, **8**, 701–706.
- 13 D. Zaguri, T. Kreiser, S. Shaham-Niv and E. Gazit, Antibodies towards Tyrosine Amyloid-Like Fibrils Allow Toxicity Modulation and Cellular Imaging of the Assemblies, *Molecules*, 2018, **23**(6), 1273, DOI: 10.3390/molecules23061273.
- 14 E. Gazit, Metabolite amyloids: a new paradigm for inborn error of metabolism disorders, *J. Inherited Metab. Dis.*, 2016, **39**, 483–488.
- 15 D. Laor, D. Sade, S. Shaham-Niv, D. Zaguri, M. Gartner, V. Basavalingappa, A. Raveh, E. Pichinuk, H. Engel, K. Iwasaki, T. Yamamoto, H. Noothalapati and E. Gazit, Fibril formation and therapeutic targeting of amyloid-like structures in a yeast model of adenine accumulation, *Nat. Commun.*, 2019, **10**, 62.
- 16 S. Auer, F. Meersman, C. M. Dobson and M. Vendruscolo, A generic mechanism of emergence of amyloid protofilaments from disordered oligomeric aggregates, *PLoS Comput. Biol.*, 2008, **4**, e1000222.
- 17 K. Stroobants, J. R. Kumita, N. J. Harris, D. Y. Chirgadze, C. M. Dobson, P. J. Booth and M. Vendruscolo, Amyloid-like Fibrils from an  $\alpha$ -Helical Transmembrane Protein, *Biochemistry*, 2017, **56**, 3225–3233.
- 18 E. Tayeb-Fligelman, O. Tabachnikov, A. Moshe, O. Goldshmidt-Tran, M. R. Sawaya, N. Coquelle, J.-P. Colletier and M. Landau, The cytotoxic Staphylococcus aureus PSM $\alpha$ 3 reveals a cross- $\alpha$  amyloid-like fibril, *Science*, 2017, **355**, 831–833.
- 19 G. Scott, A. F. Ramlackhansingh, P. Edison, P. Hellyer, J. Cole, M. Veronese, R. Leech, R. J. Greenwood, F. E. Turkheimer, S. M. Gentleman, R. A. Heckemann, P. M. Matthews, D. J. Brooks and D. J. Sharp, Amyloid pathology and axonal injury after brain trauma, *Neurology*, 2016, **86**, 821–828.
- 20 V. E. Johnson, W. Stewart and D. H. Smith, Traumatic brain injury and amyloid- $\beta$  pathology: a link to Alzheimer's disease?, *Nat. Rev. Neurosci.*, 2010, **11**, 361–370.
- 21 N. Blau, F. J. van Spronsen and H. L. Levy, Phenylketonuria, *Lancet*, 2010, **376**, 1417–1427.

- 22 K. Michals-Matalon, G. Bhatia, F. Guttler, S. K. Tyring and R. Matalon, Response of Phenylketonuria to Tetrahydrobiopterin, *J. Nutr.*, 2007, **137**, 1564S–1567S.
- 23 T. D. Douglas, A. M. Nucci, A. M. Berry, S. T. Henes and R. H. Singh, Large neutral amino acid status in association with P:T ratio and diet in adult and pediatric patients with phenylketonuria, *JIMD Rep.*, 2019, **50**, 50–59.
- 24 K. Chu, Phenylketonuria: Research and development of nutrition, *AIP Conf. Proc.*, 2020, **2208**, 20042.
- 25 V. Singh, R. K. Rai, A. Arora, N. Sinha and A. K. Thakur, Therapeutic implication of L-phenylalanine aggregation mechanism and its modulation by D-phenylalanine in phenylketonuria, *Sci. Rep.*, 2014, **4**, 3875.
- 26 A. De Luigi, A. Mariani, M. De Paola, A. Re Depaolini, L. Colombo, L. Russo, V. Rondelli, P. Brocca, L. Adler-Abramovich, E. Gazit, E. Del Favero, L. Cantù and M. Salmona, Doxycycline hinders phenylalanine fibril assemblies revealing a potential novel therapeutic approach in phenylketonuria, *Sci. Rep.*, 2015, **5**, 15902.
- 27 T. D. Do, W. M. Kincannon and M. T. Bowers, Phenylalanine Oligomers and Fibrils: The Mechanism of Assembly and the Importance of Tetramers and Counterions, *J. Am. Chem. Soc.*, 2015, **137**, 10080–10083.
- 28 H. W. German, S. Uyaver and U. H. E. Hansmann, Self-Assembly of Phenylalanine-Based Molecules, *J. Phys. Chem. A*, 2015, **119**, 1609–1615.
- 29 E. Gazit, A possible role for  $\pi$ -stacking in the self-assembly of amyloid fibrils, *FASEB J.*, 2002, **16**, 77–83.
- 30 S. Shaham-Niv, P. Rehak, D. Zaguri, A. Levin, L. Adler-Abramovich, L. Vuković, P. Král and E. Gazit, Differential inhibition of metabolite amyloid formation by generic fibrillation-modifying polyphenols, *Commun. Chem.*, 2018, **1**, 25.
- 31 D. Banik, R. Dutta, P. Banerjee, S. Kundu and N. Sarkar, Inhibition of Fibrillar Assemblies of L-Phenylalanine by Crown Ethers: A Potential Approach toward Phenylketonuria, *J. Phys. Chem. B*, 2016, **120**, 7662–7670.
- 32 P. Singh, S. K. Brar, M. Bajaj, N. Narang, V. S. Mithu, O. P. Katare, N. Wangoo and R. K. Sharma, Self-assembly of aromatic  $\alpha$ -amino acids into amyloid inspired nano/micro scaled architects, *Mater. Sci. Eng., C*, 2017, **72**, 590–600.
- 33 P. Singh, N. Narang, R. K. Sharma and N. Wangoo, Interplay of Self-Assembling Aromatic Amino Acids and Functionalized Gold Nanoparticles Generating Supramolecular Structures, *ACS Appl. Bio Mater.*, 2020, **3**, 6196–6203.
- 34 P. Singh, N. Wangoo and R. K. Sharma, Phenylalanine dimer assembly structure as the basic building block of an amyloid like photoluminescent nanofibril network, *Soft Matter*, 2020, **16**, 4105–4109.
- 35 H. K. Berry, M. K. Bofinger, M. M. Hunt, P. J. Phillips and M. B. Guilfoile, Reduction of cerebrospinal fluid phenylalanine after oral administration of valine, isoleucine, and leucine, *Pediatr. Res.*, 1982, **16**, 751–755.
- 36 C. H. Görbitz, Crystal structures of amino acids: from bond lengths in glycine to metal complexes and high-pressure polymorphs, *Crystallogr. Rev.*, 2015, **21**, 160–212.
- 37 S. Bera, S. Mondal, S. Rencus-Lazar and E. Gazit, Organization of Amino Acids into Layered Supramolecular Secondary Structures, *Acc. Chem. Res.*, 2018, **51**, 2187–2197.
- 38 J. Kyte and R. F. Doolittle, A simple method for displaying the hydropathic character of a protein, *J. Mol. Biol.*, 1982, **157**, 105–132.
- 39 J. Popot and C. De, Vitry, Integral Membrane Protein, *Encycl. Cancer*, 2011, 1884.
- 40 R. Wolfenden, L. Andersson, P. M. Cullis and C. C. B. Southgate, Affinities of Amino Acid Side Chains for Solvent Water, *Biochemistry*, 1981, **20**, 849–855.
- 41 S. Guerin, A. Stapleton, D. Chovan, R. Mouras, M. Gleeson, C. McKeown, M. R. Noor, C. Silien, F. M. F. Rhen, A. L. Kholkin, N. Liu, T. Soulimane, S. A. M. Tofail and D. Thompson, Control of piezoelectricity in amino acids by supramolecular packing, *Nat. Mater.*, 2018, **17**, 180–186.
- 42 N. Gour, C. Kanth, P. B. Koshti, V. Kshtriya, D. Shah, S. Patel, R. Agrawal-Rajput and M. K. Pandey, Amyloid-like Structures Formed by Single Amino Acid Self-Assemblies of Cysteine and Methionine, *ACS Chem. Neurosci.*, 2019, **10**, 1230–1239.
- 43 C. Bleiholder, D. B. Werz, H. Köppel and R. Gleiter, Theoretical Investigations on Chalcogen–Chalcogen Interactions: What Makes These Nonbonded Interactions Bonding?, *J. Am. Chem. Soc.*, 2006, **128**, 2666–2674.
- 44 M. R. H. Krebs, E. H. C. Bromley and A. M. Donald, The binding of thioflavin-T to amyloid fibrils: localisation and implications, *J. Struct. Biol.*, 2005, **149**, 30–37.
- 45 M. Biancalana and S. Koide, Molecular mechanism of Thioflavin-T binding to amyloid fibrils, *Biochim. Biophys. Acta, Proteins Proteomics*, 2010, **1804**, 1405–1412.
- 46 A. I. Sulatskaya, A. V. Lavysh, A. A. Maskevich, I. M. Kuznetsova and K. K. Turoverov, Thioflavin T fluoresces as excimer in highly concentrated aqueous solutions and as monomer being incorporated in amyloid fibrils, *Sci. Rep.*, 2017, **7**, 2146.
- 47 B. H. Toyama and J. S. Weissman, Amyloid structure: conformational diversity and consequences, *Annu. Rev. Biochem.*, 2011, **80**, 557–585.
- 48 P. Banerjee, A. Pyne and N. Sarkar, Understanding the Self-Assembling Behavior of Biological Building Block Molecules: A Spectroscopic and Microscopic Approach, *J. Phys. Chem. B*, 2020, **124**, 2065–2080.
- 49 Y. Zhang, V. H. Man, C. Roland and C. Sagui, Amyloid Properties of Asparagine and Glutamine in Prion-like Proteins, *ACS Chem. Neurosci.*, 2016, **7**, 576–587.
- 50 D. Pinotsi, A. K. Buell, C. M. Dobson, G. S. Kaminski Schierle and C. F. Kaminski, A Label-Free, Quantitative Assay of Amyloid Fibril Growth Based on Intrinsic Fluorescence, *ChemBioChem*, 2013, **14**, 846–850.
- 51 S. Shaham-Niv, Z. A. Arnon, D. Sade, A. Lichtenstein, E. A. Shirshin, S. Kolusheva and E. Gazit, Intrinsic Fluorescence of Metabolite Amyloids Allows Label-Free Monitoring of Their Formation and Dynamics in Live Cells, *Angew. Chem., Int. Ed.*, 2018, **57**, 12444–12447.
- 52 X. Chen, W. Luo, H. Ma, Q. Peng, W. Z. Yuan and Y. Zhang, Prevalent intrinsic emission from nonaromatic amino acids and poly(amino acids), *Sci. China: Chem.*, 2018, **61**, 351–359.